RSC Advances

ROYAL SOCIETY OF CHEMISTRY

www.rsc.org/advances

RSC Advances

PAPER

Synthesis of Hybrid Zinc/Silyl Acrylate Copolymers and their Surface Properties in the Microfouling Stage

Received 17th November 2015,
Accepted 00th January 2016

DOI: 10.1039/x0xx00000x

www.rsc.org/

Rongrong Chen, [a,b] Yakun Li, [a] Minglong Yan, [a] Xun Sun, [a] Huajing Han, [a] Jie Li, [a] Jun Wang, [a,b] Lianhe Liu, *[a,c] Kazunobu Takahashi, *[a]

Development of environmentally friendly and efficient marine antifouling coating is a central goal in marine antifouling. In this study, a series of novel hybrid zinc/silyl acrylate copolymers (Zn/Si-acrylate copolymers) composed of tri(isopropyl)silyl acrylate (TIPSA), zinc-2-ethylhexanoate methacrylate (Zn-monomer), ethyl acrylate and methyl methacrylate were synthesized and their surface compositions, thermal degradation and hydrolysis properties were investigated. After immersed in seawater, the hydrolysis of TIPSA and Zn-monomer could lead to a gradual self-peeling of the Zn/Si-acrylate surfaces, which was controlled by the ratios of TIPSA and Zn-monomer. The Zn/Si-acrylate copolymers with high Zn-monomer content showed excellent performance in the resistance of diatom *Phaeodactylum tricornutum* (*P. tricornutum*) growth on the Zn/Si-acrylate films. Both the self-peeling and release of zinc compound lead to antifouling properties, which demonstrated that Zn/Si-acrylate copolymers were effective resin for marine antifouling in static or low flow conditions.

1. Introduction

Marine biofouling, which has been an economic problem for centuries, leads to an increase in the shear drag on ships' hulls with environmental and economic penalties, accelerates the corrosion of metallic substrates and decreases the service life of marine equipment.[1, 2] Chemically active marine coatings containing tributyltin (TBT) and high cuprous oxide are effective for combating marine fouling, but they are under environmental scrutiny because they are detrimental to nontarget organisms and ecologically harmful.[3-5] As a consequence, research efforts have focused on environmentally friendly systems, such as self-polishing polymers,[6, 7] amphiphilic polymers,[8-11] zwitterionic polymers,[12, 13] biodegradable copolymers,[14, 15] and hydrogels,[16, 17] that are able to repel marine fouling organisms or minimize their adhesion to surfaces.

Among these applicable antifouling paints, self-polishing coatings with acrylate esters are one type of the most useful, effective and popular antifouling coatings. Since the worldwide prohibition of TBT for its high adverse effects on marine environments,[18] a series of zinc acrylate copolymers and triorganosilyl methacrylate-based polymers bearing hydrolysable pendant groups have been used as substitutes.[19, 20] All acrylate copolymers are initially water-insoluble and able to be hydrolyzed in seawater through an ionic exchange or hydrolysis reaction with seawater, which make them water-soluble. The hydrolysis of alkylsilyl (meth)acrylate-based polymers could give the coatings self-smoothing properties, which positively contribute to the hydrodynamics of the ship's hull by reducing the frictional drag and total amount of fuel consumed.[21] Bressy et al. first reported hydrophobic-hydrolysable copolymers consisting of methyl methacrylate (MMA) and tert-butyldimethylsilyl methacrylate (TBDMSMA) synthesized by a reversible addition-fragmentation chain transfer (RAFT) polymerization technique, and the diblock copolymers exhibited good antifouling abilities in the Mediterranean Sea for 18 months.[6, 22, 23] Hong et al. reported a novel type of self-hydrogel-generating antifouling coating made of cross-linked copolymer chains containing methyl methacrylate (MMA), acrylic acid (AA) and hydrolysable tributylsilyl methacrylate (TBSMA).[24]

These reports indicated that the leaching form of the polymers depended on the hydrolysable monomer content,[22, 25] size of the alkyl groups linked to the silicon atom,[26] molecular weight and hydrophilicity of the comonomers.[23, 27] However, the alkyl-silyl methacrylate-based paint with a low erosion rate exhibited poor antifouling ability in a static marine environment unless the alkylsilyl (meth)acrylate content was increased to over 45 wt%.[3, 28] Furthermore, the coatings with this copolymer as the binder also perform poorly against diatoms, the major component of primary colonizers or slime, which is the key step for the colonization of spores and larvae of macrofoulants including macroalgae, sponges, barnacles, bryozoans, tunicates and so on.[29, 30] This situation requires the removal of fouling with a higher speed from extensively fouled

[a] Key Laboratory of Superlight Material and Surface Technology, Ministry of Education, Harbin Engineering University, 150001, China
[b] Institute of Advanced Marine Materials, College of Materials Science and Chemical Engineering, Harbin Engineering University, Harbin 150001, China
[c] Qingdao Advanced Marine Material Technology Co., Ltd, Qingdao, 266100, China

hulls. Therefore, it is important to optimize the structure of a alkylsilyl (meth)acrylate copolymer to improve its antibiofouling ability under static or low speed conditions.

In addition, little is known about *Phaeodactylum tricornutum* (*P. tricornutum*) cell adhesion properties and the surface elements related to the hydrolysis of polymers for self-polishing antifouling coatings. In this study, a set of antifouling binders were developed to form a self-renewing and anti-diatom surface using Zn/Si-acrylate copolymers composed of different ratios of tri(isopropyl)silyl acrylate (TIPSA), zinc-2-ethylhexanoate methacrylate (Zn-monomer), ethyl acrylate (EA), and methyl methacrylate (MMA) (as shown in Scheme 1). By varying the monomer ratio of TIPSA to Zn-monomer, copolymers with a wide range of compositions could be acquired. The function of the labile ester, including organosilyl ester and zinc carboxylic ester, on the thermal degradation and hydrolysis properties were investigated and compared to the TIPSA copolymer for the first time, under the same conditions. The inhibition of the growth of diatoms and adhesion experiments showed that the Zn/Si-acrylate copolymer manifested a strong resistance to fouling.

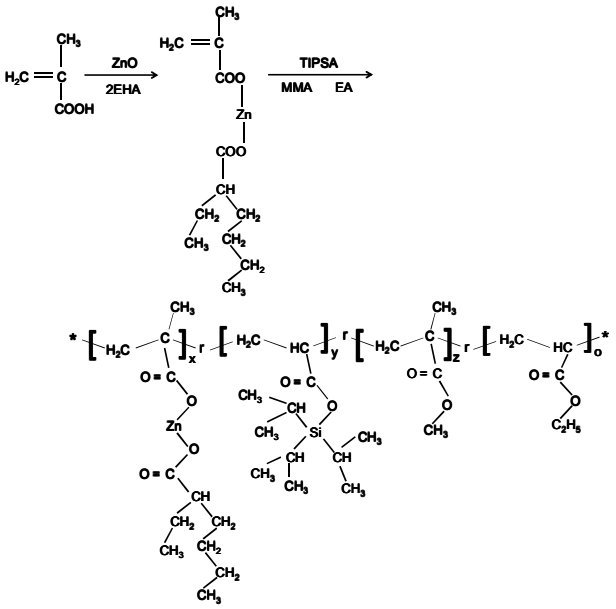

Scheme 1. Synthetic route of Zn/Si-acrylate copolymers.

2. Experimental

2.1 Materials

Xylene, 1-methoxy-2-propanol (PGM), EA, MMA, 2-ethylhexanoic acid (2EHA), methacrylic acid (MAA), and azobisisobutyronitrile (AIBN) were purchased from the Guangfu Chemical Reagent Co. (Tianjin, China). Tri(isopropyl)-silyl acrylate (TIPSA) and benzoyl peroxide (BPO) were obtained from the Shanghai Novel Technical Co. and the Shanghai Shanpu Chemical Co., respectively. Deionized water was purified with a Milli-Q Plus system (Millipore, Schwalbach, Germany). Artificial seawater (ASW) used in diatom cultivation was prepared according to ASTM D1141-98, whereas the ASW in the film immersion experiment was prepared by reef salt provided by Seachem. All reagents were used as received without further purification.

2.2 Synthesis of the copolymer resin

Zn/Si-acrylate copolymers were synthesized by a two-step method as shown in Scheme 1. First, ZnO, MAA and 2EHA were used to synthesis Zn-monomer by an acid-base reaction; then, Zn/Si-acrylate copolymers were prepared via radical copolymerization initiated by AIBN and BPO. AIBN was dissolved with the monomers and initiated polymerization in the first stage and BPO was added in the second stage to increase the monomer conversion degree as chaser.

2.2.1 Synthesis of the Zn-monomer

Into a four-necked flask equipped with a cooling tube, thermometer, dropping funnel and stirrer, 170.8 parts of PGM and 81.4 parts of ZnO were charged, and the mixture was heated up to 75 °C while stirring. Then, a mixture of 86.1 parts of MAA, 144.2 parts of 2EHA and 10 parts of water was added dropwise from the dropping funnel over 3 hours at a constant speed. After completion of addition, the reaction solution changed from opaque to transparent. Finally, the solution was stirred for 2 hours, and then 95 parts of PGM was added to obtain a transparent metal-containing monomer dissolved mixture (Zn-monomer). The solid content and acid value were approximately 50.0% and 381.4 mgKOH·g^{-1}, respectively. ^{1}H NMR (500 MHz, $CDCl_3$, ppm): 5.48-6.25 (C***H***$_2$CH(CH$_3$)), 1.86 (CH$_2$CH(C***H***$_3$)), 1.01−1.30 (C***H***(C***H***$_2$C***H***$_3$)(C***H***$_2$C***H***$_2$C***H***$_2$C***H***$_3$)). IR: 2860 (CH$_2$), 1730 (C=O), 1600 (O=C-O).

2.2.2 Synthesis of Zn/Si-acrylate copolymers

Considering the real applications, the copolymers were synthesized by free radical polymerization. Typical reaction conditions are as follows: a mixture of 57 parts of xylene and 15 parts of PGM was first placed in a 4-necked flask equipped with an agitator, a reflux condenser, a thermometer and a dropping funnel. The solvent was heated to 90-95 °C under nitrogen, and then a transparent mixture of MMA, EA, TIPSA, Zn-monomer and 1.5 parts of AIBN was added dropwise into the flask at a constant speed over a 3 h period. After completion of the addition, 0.5 parts of BPO and 10 parts of xylene were added dropwise over 30 minutes, and the mixture was further stirred for 2.5 hours. Then, some parts of xylene were added to obtain a slightly turbid pale metal-containing resin having a heated residue proportion of 45.0%. Table 1 summarizes the compositions and molecular characterization of the Zn/Si-acrylate copolymers, and it also gives the assignment of sample abbreviations. The Mn and PDI of Zn/Si-acrylate copolymers determined by gel permeation chromatography (GPC) are in the range 1.2×10^3-1.5×10^4 g/mol and 1.1-2.4, respectively. ^{1}H NMR (500 MHz, $CDCl_3$, ppm): 3.95-4.20 (C***H***COOC***H***$_2$CH$_3$), 1.01−1.30 (CHCOOCH$_2$C***H***$_3$), 1.01−1.30 (CC***H***$_3$COOCH$_3$), 3.60−3.67 (CCH$_3$COOC***H***$_3$), 1.01−1.30 (C***H*** (C***H***$_2$C***H***$_3$)(C***H***$_2$C***H***$_2$C***H***$_2$C***H***$_3$)), 1.27 (SiC***H***(CH$_3$)$_2$), 1.10 (SiCH(C***H***$_3$)$_2$). IR: 2860 (CH$_2$), 1730 (C=O), 883 (Si−C) cm^{-1}.

Table 1. Compositions and molecular characterization of the Zn/Si-acrylate copolymers

Sample	MMA/EA/TIPSA/Zn-monomer [a]	Mn[b]/ g·mol^{-1}	PDI	Conversion/%
Si-polymer	10/52/38/0	—	—	96
Zn/Si-1	10/52/34/4	1,200	1.09	95
Zn/Si-2	10/52/31/7	3,200	2.43	92
Zn/Si-3	10/52/28/10	5,000	1.76	83
Zn/Si-4	10/52/25/13	3,700	2.22	95
Zn/Si-5	10/52/22/16	—	—	—
Zn/Si-6	10/52/19/19	14,900	2.34	—

[a] Feed weight ratio.

[b] Determined by GPC with PS standards.

2.3 Characterization

2.3.1 FTIR. The FTIR spectra of the polymer films on potassium bromide plates cast from solutions were collected using a Perkin Elmer Spectrum 100 Fourier transform infrared (FTIR) spectrometer.

2.3.2 GPC. The molecular weights and molecular weight distributions (Mn and PDI) of the copolymers were measured on a Waters 1515 gel permeation chromatography (GPC) apparatus (with THF as the eluent at a flow rate of 0.4 mL/min at 35 °C). The instrument was calibrated with polystyrene (PS) standards (400- 43000 g/mol).

2.3.3 ^{1}H NMR spectroscopy. ^{1}H NMR spectra (500 MHz) were recorded on a Bruker AVANCE III-500 instrument using $CDCl_3$ as the solvent at room temperature.

2.3.4 Thermal analysis. Thermogravimetric analysis (TGA) was performed on a TA Q50 instrument under a nitrogen atmosphere at a heating rate of 20°C/min in the range of 30–500°C. The thermogravimetric weight loss curve (TG, %) and the weight loss derivative curve (DTG, %/°C) were recorded as a function of the temperature.

2.3.5 XPS and SEM. The chemical state of the substrate's surface was evaluated by X-ray photoelectron analysis on a multi-functional X-ray photoelectron spectroscopy (XPS) instrument (PHI-5700, Perkin-Elmer, USA). The scanning electron microscopy (SEM) study was performed using a JEOL JSM-6480A microscope equipped with a spectrometer for energy-dispersive X-ray spectroscopy (EDS).

2.4 Biofouling assays

The diatom, *P. tricornutum* ACCC 01625 was obtained from the Center for Collections of Marine Algae of Xiamen University (CCMA), Pearl River Estuary, China. Cells were cultured in F/2 medium without aeration at 21±2°C with a 12:12 h light: dark (L/D) cycle of fluorescent illumination at 2000 lux,[31] and they were gently stirred twice daily. A log-phase suspension of cells was found to have a cell number of approximately 10^5 cells/mL. One hundred mL of cell suspension was added to individual conical flasks, each containing a test slide, prepared as described above. The microalgae cell concentration was counted on a cell count chamber hemocytometer with an optical microscope (Leica DML 300B, Germany) and correlated to the optical densities at 314.5 nm of the microalgae samples based on linear fitting equations. For every period, the micro-algal density was quantified via a UV-2550-Visible Spectrophotometer (SHIMADZU Corporation, Japan). All of the experiments were carried out in three replicates. The error bars correspond to the average standard deviations. The cells attached to the surfaces were observed using an optical microscope (Leica dmi 300B).

2.5 Weight-loss measurement.

To measure the self-peeling rates, each dried coated glass slide was weighed (w_0) before dipping into a tank of artificial seawater (ASW) at 21.6±1°C that was changed every week. After different time periods, the glass slides were taken out from the ASW, immersed in distilled water for 4 h and then gently dried at room temperature before their weights ($w_{t,wet}$) were recorded. Then, all of these glass slides were dried at 100°C for 6 h before their weights ($w_{t,dry}$) were recorded. The weight difference between $w_{t,wet}$ and w_0 reflects the water adsorption of each coating, whereas the weight difference between $w_{t,wet}$ and $w_{t,dry}$ shows the weight-loss (self-polishing or self-peeling) of water in each coating's leaching layer. For each resin, three coated glass slides were prepared and tested. Therefore, each result reported and used hereafter was averaged over three identical coatings. The mass loss (%) was calculated from eqn. (1):

$$\text{mass loss} = \frac{w_t - w_0}{w_0 - w_{panel}} \quad (1)$$

where $\mathbf{w_t}$, $\mathbf{w_0}$ and $\mathbf{w_{panel}}$ are the weights of the coated panel at time t, the coated panel at time t = 0 and the initial non-coated panel, respectively.

3. Results and discussion

3.1 The chemical compositions of the Zn/Si-acrylate copolymers

In the present work, Zn/Si-acrylate copolymers were synthesized by a two-step method as shown in Scheme 1. The Zn-monomer was first synthesized and copolymerized with TIPSA and other monomers. The chemical structures of Zn-monomer, TIPSA, Si-polymer and Zn/Si-acrylate copolymers by FT-IR spectra are shown in Fig. 1. The peaks at 1630-1620 cm^{-1} and 880 cm^{-1} (Fig. 1a) were ascribed to the stretching vibrations of the C=C and Si-C bonds, respectively. The peak intensity of the C=C bonds in copolymers decreased significantly compared to that in monomers (Fig. 1b), whereas the peak at 1730 cm^{-1} corresponding to the carbonyl group of ester bonds in the Zn/Si-acrylate copolymer chains was observed. Comparing the spectrum of Si-polymer with that of Zn/Si-acrylate copolymers, we can find that the asymmetrical stretching vibration of the carboxylic group showed a peak at approximately 1600 cm^{-1}. The relative intensities of 1600 cm^{-1} and 800 cm^{-1} increased with the Zn-monomer and TIPSA content, respectively. These results suggested that the TIPSA monomer and Zn-monomer were copolymerized.

Fig. 2 illustrates the TG and DTGA curves of Si-polymer and hybrid Zn/Si-acrylate copolymers at a heating rate of 20 K/min

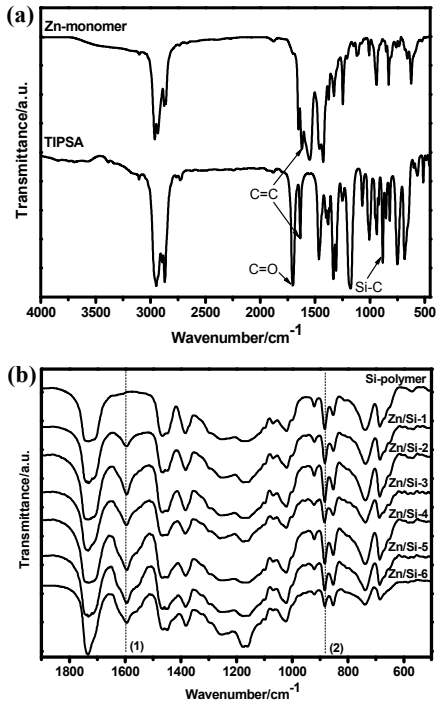

Figure 1. FTIR spectra of the Zn-monomer and TIPSA (a). FTIR spectra of Si-polymer and Zn/Si-acrylate copolymers (b). (1) 1600 cm^{-1}, (2) 880 cm^{-1}.

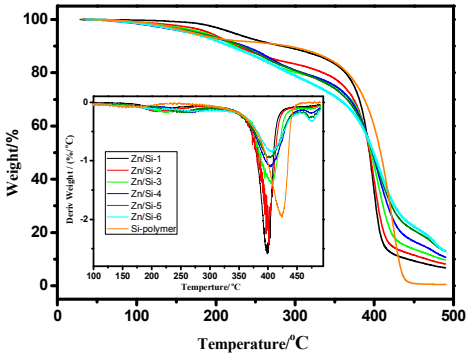

Figure 2. TGA and DTGA (the inset) curves of hybrid Zn/Si-acrylate copolymers.

under an inert atmosphere. The Si-polymer exhibits only a main decomposition at high temperature from 350 to 440°C. However, for Zn/Si-acrylate copolymer samples, three weight loss stages were encountered in the thermal degradation, with a main decomposition, which occurred from 350 to 450°C. A first weak degradation stage and the third stage of weight loss were recorded from 180 to 310°C and from 455 to 490°C, respectively. Compared with Si-acrylate copolymers and previous related reports, the first slight DTG peak from approximately 207 to 270°C would correspond to the degradation initiated by a radical transfer to the unsaturated chain. The second well-resolved sharp peaks between 395 and 425°C could be indicative of a degradation initiated from the random C-C scission of the backbone for Zn/Si- and Si-acrylate copolymers.[15, 23, 32] The third stage of Zn/Si-acrylate co-polymers thermal degradation at 475°C would correspond to the random chain scission of methacrylic acid zinc salt saturated polymer chains because the depropagation rate is in keeping with the content of the carboxylic acid metal salt component. Compared with Si-polymer, these hybrid Zn/Si-acrylate copolymers produced significant amounts of residual char in nitrogen in 490°C due to the existence of Zn-monomer. Therefore, all the information indicated that the TIPSA monomer was successfully copolymerized with Zn-monomer in the reaction.

3.2 Hydrolysis of Zn/Si-acrylate copolymers

Fig. 3 shows the immersion-time dependence of the mass loss of Zn/Si-acrylate copolymers in artificial seawater under static conditions. Both the wet mass loss (Fig. 3a) and dry mass loss (Fig. 3b) display similar trends. The films with different molar proportions of hydrolysable units within the macromolecular chains behave similarly, indicating that at the initial stage (approximately 445 h), all of the films tested start to lose weight. After approximately 400 h of immersion, the weight loss rates of all of the films become stable. Both the relative weight loss of the hybrid coatings and the self-peeling rate (the slope) all increase with the Zn-monomer content. According to the report [20], the amount of zinc acrylate and the type of the alkyl groups in the acrylic ester comonomers had the most significant influence on the leaching of the polymers together. This may be because the Zn-monomer in the acrylate copolymers has a higher hydrolysis rate than TIPSA, which makes those copolymer chains on the top layer soluble so that they are washed away at a faster rate. In comparison with cross-linked terpolymer with hydrolyzable tributylsilyl methacrylate (TBSM) or triisopropylsilyl methacrylate (TIPSM)[7], the Zn/Si-acrylate films lost more weight than cross-linked terpolymer after immersion, which is due to that fact that TIPSA has a higher hydrolysis rate than TBSM or TIPSM. The higher self-peeling process could lead to an excellent antifouling property in static water environment.

Fig. 3c showed the mass loss differences of the wet weight and dry weight of Si- and Zn/Si-acrylate copolymers for different immersion times. Within the initial 250 h, the mass loss difference of wet weight and dry weight decreased sharply, and the situation tended to steady after 250 h. For a random copolymer, the zinc and silyl monomer units were statistically distributed all along the macromolecular chains with a slight deviation in the molar composition during the polymerization, as previously reported.[33] The formation of carboxylate ions could occur uniformly and result in the hydrolyzed polymer. The mass loss difference indicated the quantity of water absorption of the hydrophilic surface layers which were made by the hydrolysis of Zn-monomer and TIPSA. The initial water absorption led to the swelling of the top layer of each film to form a hydrogel and not the dissolution in ASW for the long chain. The average mass loss difference after 250 h of immersion in ASW increased with the Zn-monomer content from 0.005% to 0.02% (Fig. 3d). Concretely, the water content trapped in films increased linearly with the increase in the Zn-monomer molar content to 5% and the decrease in the silyl

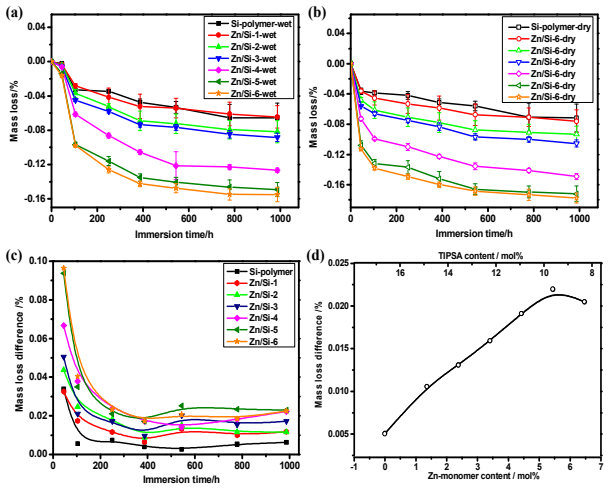

Figure 3. Immersion-time dependence of the mass loss of Zn/Si-acrylate copolymers in ASW, where each coating was prepared on a glass slide with dimensions of 25 x 58 mm^2. (a) The wet weight curve, (b) the dry weight curve, (c) the mass loss difference of wet weight and dry weight and (d) the average mass loss difference dependence (after 250 h) of the Zn-monomer content.

acrylate monomer from 16.6 to 9.6%. Meanwhile, when the Zn-monomer content is over 5.5%, the absorption began to decrease. The results indicated that the hydrolysis of Zn-monomer could accommodate more amount water than TIPSA monomer in the leached layers, and also provided higher weight loss of the polymers combined with the result of Fig. 3a and Fig. 3b. This suggested that the hydrolysis of TIPSA and Zn-monomer eventually made a thin hydrophilic surface layer, which is gradually dissolved and washed away, further exposing the inner layer to sea water when the polymer surface is immersed in seawater. Therefore, the balance between the hydrolysis and dissolution of the Zn/Si-acrylate copolymer is critical.

No studies have been devoted to the hydrolysis/ionic exchange reaction of hybrid Zn/Si-acrylate copolymers. The synthesized Zn/Si-acrylate copolymers were fabricated into flat films via the membrane scraper. Fig. 4 shows the EDS analysis of the surfaces of the Si-polymer and the Zn/Si-acrylate co-

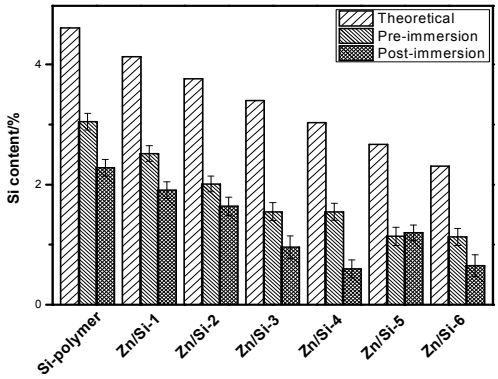

Figure 4. Contents of Si on the Zn/Si-acrylate copolymer surfaces measured by EDS.

polymers pre- and post-immersion in the diatom solution. A comparison of the experimental EDS composition data of the copolymers with the theoretical values demonstrates that the surface is not dominated by the tri(isopropyl)silyl moieties for the short side chains and homopolymerization of all of the monomers. The chemical compositions of the Zn/Si-acrylate copolymer surfaces immersed in the diatom solution showed lower elemental Si contents.

To obtain more information about these hydrolysable surfaces, XPS analysis was used to determine the chemical composition and nature of the chemical bonding on the surfaces. Fig. 5 shows the X-ray photoelectron spectra (XPS) of pristine Si-acrylate and Zn/Si-acrylate films as well as their higher resolution spectra of the C 1s areas. The binding energies in the XPS experiment were corrected by referencing the C1s peak to 284.6 eV. In the XPS wide-scan spectra of the pristine Si-polymer (Fig. 5a) and Zn/Si-3 film (Fig. 5c), the Si 2p and Si 2s signals with respective biding energies (BEs) of approximately 99 and 151 eV are associated with alkoxysilanes and their elemental composition. The depicted elemental Zn with binding energies at approximately 1022 and 1045 eV shown as an inset in Fig. 5c indicates the successful copolymerization of Zn-monomer and TIPSA.[34] These results agreed well with the EDS data and demonstrated a decrease in the silicon and Zn atoms within the surface prior to the immersion. The C 1s core-level spectrum of pristine Si-polymer (Fig. 5b) can be fitted into four components: The main peak at 284.6 eV was due to carbon bound only to carbon and hydrogen (C–H/C–C); the other three fitted peaks were attributed to the component O-C=O (i.e., carboxylic esters) species at 288.4 eV, C–O species at 286.2 eV and Si-C species at 283.9 eV.[35, 36] The area ratios of the four peak components [C=O]:[C-O]:[C-H]:[C-Si] are approximately 1:1.2:4.8:0.5 and 1:1.0:5.8:0.3, which are consistent with the theoretical ratios of the Si-polymer and Zn/Si-acrylate copolymers.

In comparison to the wide scan spectrum of the pristine surface (Fig. 5ac), the weak Cl 2p (at the BE of approximately 209 eV), Na 1s (at the BE of approximately 1078 eV) and N 1s (at the BE of approximately 400 eV) signals appear in the wide scan spectra of the Zn/Si-acrylate surfaces (Fig. 6ac), which may be caused by the absorption of the ions in artificial seawater. The C 1s core-level spectra of pristine Si-polymer and Zn/Si-3 (Fig. 6bd) can be curve-fitted into three peak components with BEs at approximately 288.4, 286.2 and 284.6 eV, attributable to the O-C=O (i.e., carboxylic acid and esters), C-O and C-H species, respectively. The area ratios of the three peak components [C=O]:[C-O]:[C-H] are approximately 1:1.8:3.6 and 1:1.4:4.7, which indicated a decrease in the carbonyl groups. Additionally, in the post-immersed surfaces, Si-C species were not detected at 283.9 eV.

Thus, the degradation (weight loss) speed of the coating is mainly controlled by both the contents of TIPSA and Zn-monomer, which can significantly improve the dissolution after hydrolysis, leading to enhanced antibiofouling in static marine environments. It is also important to note that in our design,

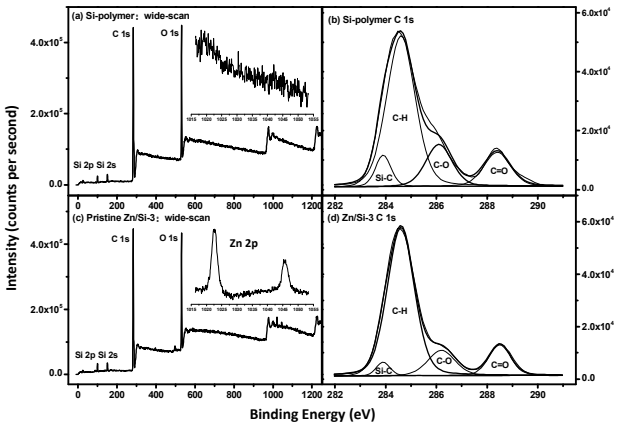

Figure 5. Survey curves of (a) pristine Si-polymer (inset: the higher resolution curves of the Zn area) and its higher resolution curves of C 1s (b), (c) pristine Zn/Si-3 (inset: the higher resolution curves of the Zn area) and its higher resolution curves of C 1s (d).

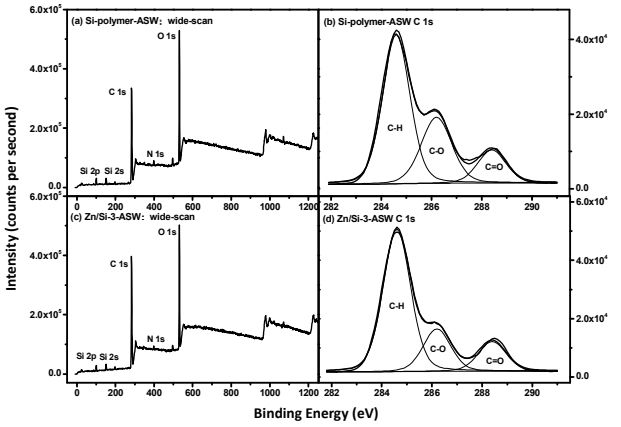

Figure 6. Survey curves of (a) Si-polymer immersed in ASW, its higher resolution curves of C 1s (b), (c) Zn/Si-3 immersed in ASW and its higher resolution curves of C 1s (d).

the degradation products released into seawater are mainly fragmented poly(methyl methacrylate) with some anionic carboxylate groups, triisopropylsilyl cations and PMMA-EA copolymer chains. To the best of our knowledge, they are not harmful and are nontoxic in marine environments.

3.3 Diatom growth inhibition and adhesion assays

Diatoms are a major component of microbial slimes that develop on man-made surfaces placed in marine environments.[37] Generally, the biofouling starts from the adhesion of bacteria, diatoms and other microalgae on the artificial surfaces immersed in the marine environment. Therefore, the diatom *P. tricornutum* was used to evaluate the antifouling character of the Zn/Si-acrylate copolymer surfaces. The effect of Zn/Si-acrylate copolymers on the inhibition of growth was evaluated in the *P. tricornutum* suspension. Fig. 7 shows the number of diatom cells in the suspension with different Zn/Si-acrylate copolymers after cultivation for 5, 19, 24, 48, 72 120 and 168 h. All of the polymer surfaces have a growth inhibitory behavior as the blank sample showed the highest cell density. It was observed that the growth rate of the diatom declined with an increase in the Zn-monomer

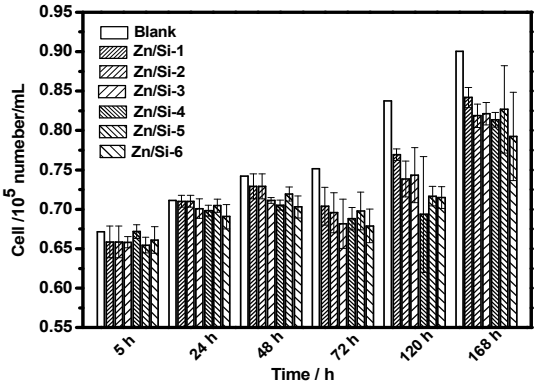

Figure 7. Density of the diatom in the solutions with various Zn/Si-acrylate copolymer films.

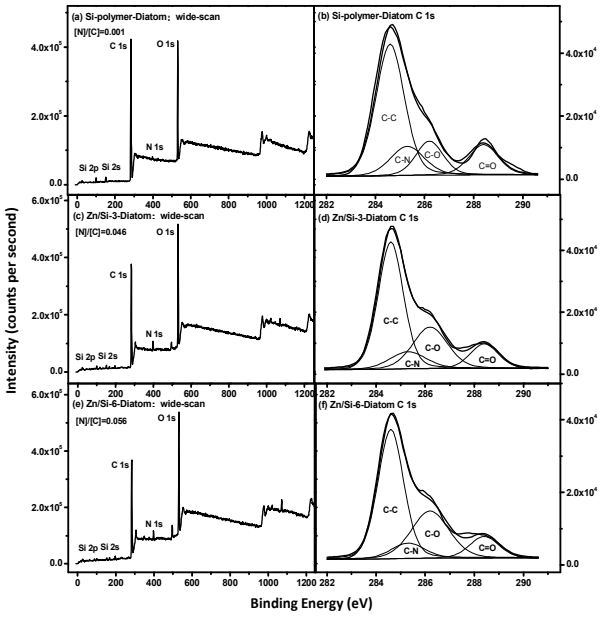

Figure 8. XPS wide scan and C 1s core-level spectra of (a, b) Si-polymer, (c, d) Zn/Si-3 and (e, f) Zn/Si-6 immersed in the diatom solution.

content, which may be due to the fragment with some anionic carboxylate groups and the zinc-2-ethylhexanoic cation.

The XPS wide scan spectra of Si-polymer, Zn/Si-3 and Zn/Si-6 surfaces after 15 d of exposure to the *P. tricornutum* cell solution and 30 min in a deionized water bath are shown in Fig. 8. The weak N 1s signals appear in the wide scan spectra of the Zn/Si-acrylate surfaces (Fig. 8ace), which are suspected to be caused by the absorption of elemental N from substitute ocean water, F/2 culture medium or the exocellular polysaccharides, which may act as metal chelating ligands and were produced to alleviate metal stress.[38] The [N]:[C] ratio, determined from the N1s and C1s core-level peak area ratio, is used to indicate the relative amounts of nitrate and proteins adsorbed on the surface.[39] From the comparison of the XPS wide-scan spectra, the relative intensity of the N 1s signal of the Zn/Si-acrylate surface is much stronger than that of the Si-polymer surface. Quantitative peak analysis showed that the

[N]:[C] molar ratio at the Zn/Si-6 surface is 0.056, in comparison with that at the Si-polymer surface, which is 0.001. This increase is probably due to Zn complexation with native EPS cells in the extracellular polymeric substance (EPS) Zn/Si-acrylate copolymer surface and the rough surfaces of Zn/Si-acrylate films.[34] Although the Si-polymer surface has little effect on the inhibition of the growth of diatoms, it also has a weak adhesion effect for the exocellular polysaccharides.

The XPS C1s core-level spectra of the Si-polymer, Zn/Si-3 and Zn/Si-6 surfaces can be curve-fitted into four peak components with BEs of approximately 284.6, 285.6, 286.2 and 288.4 eV (Fig. 8bdf), which are attributable to the C-H, C-N, C-O, and C=O species, respectively.[40, 41] From the quantitative changes in the peak area ratios, it can be seen that the contents of O=C-O groups on surfaces that were immersed in artificial seawater and the diatom solution are less than the as-prepared surface. This result demonstrates that O=C-O groups in the methacrylic acid zinc salt component and carboxylic silyl ester component decreased in the artificial seawater. According to Fig. 5, Fig. 6 and Fig. 8, we can discover that in both the artificial seawater and diatom solution, the O=C-O groups and C–O bonds appeared on the reacted surfaces. This finding is in good agreement with the hydrolysis, i.e., the surface of which is mainly occupied by carbonyl moieties. Due to a hydrolysis/ionic exchange reaction with seawater, the zinc- and trialkylsilyl-pendant groups will be cut off from the backbone. Thus, based on the XPS analysis, we could deduce that both the methacrylic acid zinc salt component and carboxylic acid silyl ester component are changed in the seawater medium, especially in a diatom solution. A conclusion can be drawn that two factors, the hydrolysable monomer type and the content of this monomer in the copolymers, are crucial in the preparation of copolymer films with controlled hydrolyzed antifouling polymer.

P. tricornutum cells, unlike the spores of Ulva, are not motile in the water column. The cells come into contact with a surface by gravity and water currents. Therefore, approximately the same number of diatoms will be in contact with all test surfaces during the incubation period. Fig. 9 shows the optical microscopy images of thin films of Zn/Si-acrylate copolymer (Fig. 9a-f) immersed in the suspension after 10 d and images of the test diatom with predominantly a fusiform morphology (Fig. 9g). There were no obvious P. tricornutum cells adhered to the surfaces in the microscope field (Fig. 9a-d). In this regard, the self-peeling surfaces with an amount of free water may preclude adsorption in proteins and self-refresh changes, and therefore, they are responsible for the low cell adhesion. The difficult to find magnified images (Fig. 9e-g) showed that the Zn/Si-6 surface has fewer adhered diatoms than the Zn/Si-1 surface, although it has a high [N]:[C] molar ratio. This means that there was a significant correlation between the zinc monomer content and the adhesion of diatom cells, even though the hydrolyzed zinc compound was not considered to be the antifouling biocide.

After seawater exposure, the tri(isopropyl)silyl ester bonds and the Zn-monomer in the top layer of each coating were

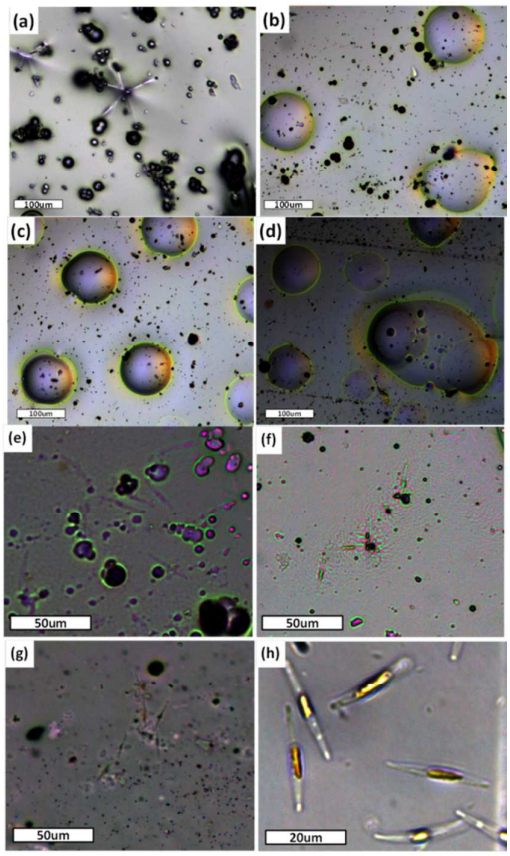

Figure 9. Optical microscopy images of thin films (a) Zn/Si-1, (b) Zn/Si-4, (c) Zn/Si-5, (d) Zn/Si-6 and the magnified images of (e) Zn/Si-1, (f) Zn/Si-5, (g) Zn/Si-6 immersed in the suspension after ten days, and (h) *P. tricornutum*.

gradually hydrolyzed into anionic and hydrophilic carboxylic groups to form a thin layer of hydrogel. However, it is important to note here that the Zn/Si-acrylate copolymers have more bubbles with an increase in the Zn-monomer content, which may be caused by the Zn-monomer hydrolysis of the top layer, which makes the polymer chains more hydrophilic (Fig. 9bcd). After a sufficient number of bonds are broken, the hydrolyzed copolymer chains, together with the hydrolysable silyl-gels and zinc-compound, are gradually dissolved into the sea water and washed away. In such a way, the next layer of polymer will be exposed to seawater so that the hydrolyzation processes continues to prevent/reduce the settlement and biofouling of marine animals on such a surface coating. This result agreed well with the hydrolysis rate. Therefore, it is vitally important to balance the hydrolysis rate to avoid an increase in surface roughness by varying the hydrolysable monomer content and type.

Conclusions

A new type of antifouling Zn/Si-acrylate copolymers composed of tri(isopropyl)silyl acrylate, zinc-2-ethylhexanoate meth-acrylate, ethyl acrylate and methyl methacrylate have been successfully developed by the combination of anti-diatom and self-peeling properties. All of the copolymers exhibited good

film forming and erosion properties in artificial seawater, making them suitable as new polymeric binders for hybrid self-polishing coatings. The gradual hydrolytic degradation can effectively slow down the fouling by the diatom. The hybrid self-generating and self-antimicroalgae idea has been conceptually proven in the current study. The newly developed copolymers have better chemical processabilities and can be readily coated onto large objects or objects with complicated geometries by a conventional method such as brushing, spraying or dipping. Moreover, the combination of these two monomers reduces the amount of expensive TIPSA required. This study highlights the developed cost-effective and environmentally friendly antifouling polymer has great potential for industrial applications.

Acknowledgements

The work was supported by the International S&T Cooperation Program of China (ISTCP) (No. 2013DFA50480), the Fundamental Research Funds of the Central University (HEUCF20151008) and the National College Students' Innovative Training Program.

Notes and references

1. M. P. Schultz, *Biofouling*, 2007, **23**, 331-341.
2. A. Lindholdt, K. Dam-Johansen, S. M. Olsen, D. M. Yebra and S. Kiil, *Journal of Coatings Technology and Research*, 2015, **12**, 415-444.
3. D. M. Yebra, S. Kiil and K. Dam-Johansen, *Progress in Organic Coatings*, 2004, **50**, 75-104.
4. A. C. A. Sousa, M. R. Pastorinho, S. Takahashi and S. Tanabe, *Environmental Chemistry Letters*, 2014, **12**, 117-137.
5. J. B. Lindén, M. Larsson, B. R. Coad, W. M. Skinner and M. Nydén, *RSC Advances*, 2014, **4**, 25063-25066.
6. C. Bressy, C. Hellio, M. N. Nguyen, B. Tanguy, J. P. Maréchal and A. Margaillan, *Progress in Organic Coatings*, 2014, **77**, 665-673.
7. F. Hong, L. Y. Xie, C. X. He, J. H. Liu, G. Z. Zhang and C. Wu, *Polymer*, 2013, **54**, 2966-2972.
8. D. R. Calabrese, B. Wenning, J. A. Finlay, M. E. Callow, J. A. Callow, D. Fischer and C. K. Ober, *Polymers for Advanced Technologies*, 2015.
9. H. S. Sundaram, Y. Cho, M. D. Dimitriou, J. A. Finlay, G. Cone, S. Williams, D. Handlin, J. Gatto, M. E. Callow, J. A. Callow, E. J. Kramer and C. K. Ober, *ACS Appl Mater Interfaces*, 2011, **3**, 3366-3374.
10. E. Martinelli, M. K. Sarvothaman, G. Galli, M. E. Pettitt, M. E. Callow, J. A. Callow, S. L. Conlan, A. S. Clare, A. B. Sugiharto, C. Davies and D. Williams, *Biofouling*, 2012, **28**, 571-582.
11. Y. J. Cho, H. S. Sundaram, C. J. Weinman, M. Y. Paik, M. D. Dimitriou, J. A. Finlay, M. E. Callow, J. A. Callow, E. J. Kramer and C. K. Ober, *Macromolecules*, 2011, **44**, 4783-4792.
12. C. J. Huang, N. D. Brault, Y. T. Li, Q. M. Yu and S. Y. Jiang, *Advanced Materials*, 2012, **24**, 1834-1837.
13. L. Mi and S. Y. Jiang, *Angew. Chem.-Int. Edit.*, 2014, **53**, 1746-1754.
14. F. Fay, I. Linossier, V. Langlois, E. Renard and K. Vallee-Rehel, *Biomacromolecules*, 2006, **7**, 851-857.
15. W. T. Xu, C. F. Ma, J. L. Ma, T. S. Gan and G. Z. Zhang, *ACS Appl Mater Interfaces*, 2014, **6**, 4017-4024.
16. L. L. Xue, X. L. Lu, H. Wei, P. Long, J. Xu and Y. F. Zheng, *J Colloid Interf Sci*, 2014, **421**, 178-183.
17. T. Murosaki, N. Ahmed and J. P. Gong, *Sci Technol Adv Mat*, 2011, **12**.
18. H. P. H. Arp, E. Eek, A. W. Nybakk, T. Glette, T. Møskeland and A. Pettersen, *Water research*, 2014, **65**, 213-223.
19. Y. Yonehara, H. Yamashita, C. Kawamura and K. Itoh, *Progress in Organic Coatings*, 2001, **42**, 150-158.
20. P. Durand, A. Margaillan, M. Camail and J. Vernet, *Polymer*, 1994, **35**, 4392-4396.
21. S. Mirabedini, S. Pazoki, M. Esfandeh, M. Mohseni and Z. Akbari, *Progress in organic coatings*, 2006, **57**, 421-429.
22. C. Bressy, M. N. Nguyen, B. Tanguy, V. G. Ngo and A. Margaillan, *Polymer Degradation and Stability*, 2010, **95**, 1260-1268.
23. C. Bressy, V. G. Ngo and A. Margaillan, *Polymer Degradation and Stability*, 2013, **98**, 115-121.
24. F. Hong, L. Xie, C. He, J. Liu, G. Zhang and C. Wu, *Journal of Materials Chemistry B*, 2013, **1**, 2048-2055.
25. M. N. Nguyen, C. Bressy and A. Margaillan, *Journal of Polymer Science Part A: Polymer Chemistry*, 2005, **43**, 5680-5689.
26. C. Bressy, A. Margaillan, F. Faÿ, I. Linossier and K. Rehel, *Advances in Marine Antifouling Coatings and Technologies, Woodhead Publishing, Cambridge, UK*, 2009, 445-491.
27. M. Lejars, A. Margaillan and C. Bressy, *Polymer Chemistry*, 2013, **4**, 3282.
28. C. Hellio and D. M. Yebra, *Advances in marine antifouling coatings and technologies*, Elsevier, 2009.
29. M. Salta, J. A. Wharton, Y. Blache, K. R. Stokes and J. F. Briand, *Environmental microbiology*, 2013, **15**, 2879-2893.
30. M. Lejars, A. Margaillan and C. Bressy, *Chem Rev*, 2012, **112**, 4347-4390.
31. R. R. Guillard and J. H. Ryther, *Canadian journal of microbiology*, 1962, **8**, 229-239.
32. M. Ferriol, A. Gentilhomme, M. Cochez, N. Oget and J. Mieloszynski, *Polymer degradation and stability*, 2003, **79**, 271-281.
33. M. N. Nguyen, C. Bressy and A. Margaillan, *Polymer*, 2009, **50**, 3086-3094.
34. X. F. Sun, S. G. Wang, X. M. Zhang, J. Paul Chen, X.-M. Li, B.-Y. Gao and Y. Ma, *J Colloid Interf Sci*, 2009, **335**, 11-17.
35. G. Beamson and D. Briggs, John Wiley & Sons New York, 1992, pp. 128–131.
36. W. Yu, E. T. Kang, K. G. Neoh and S. Zhu, *The Journal of Physical Chemistry B*, 2003, **107**, 10198-10205.
37. P. J. Molino and R. Wetherbee, *Biofouling*, 2008, **24**, 365-379.
38. S. K. Kawakami, M. Gledhill and E. P. Achterberg, *Biometals*, 2006, **19**, 51-60.
39. W. J. Yang, T. Cai, K.-G. Neoh, E.-T. Kang, G. H. Dickinson, S. L.-M. Teo and D. Rittschof, *Langmuir : the ACS journal of surfaces and colloids*, 2011, **27**, 7065-7076.
40. D. Pranantyo, L. Q. Xu, K. G. Neoh, E. T. Kang, W. Yang and S. L. M. Teo, *Journal of Materials Chemistry B*, 2014, **2**, 398-408.
41. B. Tesson, M. J. Genet, V. Fernandez, S. Degand, P. G. Rouxhet and V. Martin‐Jézéquel, *ChemBioChem*, 2009, **10**, 2011-2024.

Graphical Abstract